Supplemental material

Puleo et al., https://doi.org/10.1083/jcb.201902101

Provided online are three tables in Excel. Table S1 shows confirmed sequences of shResist EVL, shResist EVL domain deletion mutants, and shResist EVL chimeric mutants. Table S2 shows the exact P values from the indicated figures. Table S3 shows the exact P values from all two-way comparisons in the indicated figures.

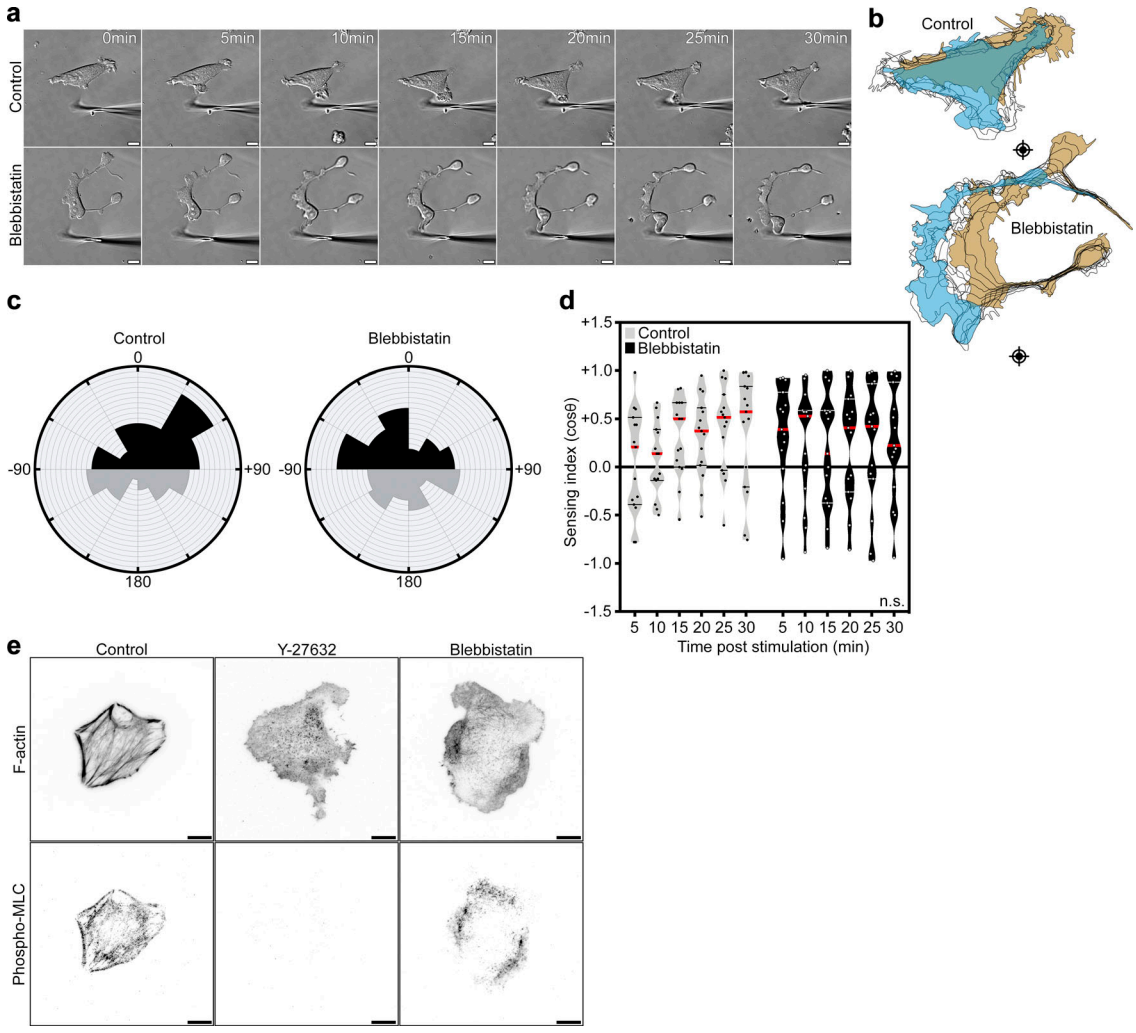

Figure S1. **Mechanically directed motility occurs under myosin suppression. (a–d)** Control (no drug) and Blebbistatin (10 µM)-treated MCF7 cells, plated on 35-kPa hydrogels, were mechanically stimulated. **(a)** Still images from representative time-lapse videos of control and Blebbistatin-treated cells (Video 2). Scale bars are 10 µm. **(b)** Corresponding cell traces at 0, 5, 10, 15, 20, 25, and 30 min, with starting positions in tan and final positions in blue. Crosshairs denote micropipette positions. **(c)** Rose plots show cumulative turning angles for control and Blebbistatin-treated cells. Black sectors denote turns in the direction of the mechanical stimulus, and gray sectors denote turns away from the mechanical stimulus. Data are collected from five independent experiments (n = 15 per condition). **(d)** Sensing indices of control and Blebbistatin-treated cells over time. Two-way ANOVA shows no significant difference in sensing index (P = 0.7761). Data are collected from five independent experiments; all data points are shown (n = 15 per condition; violin plot shows median and quartiles of sensing indices). **(e)** Representative inverted TIRF images of control (no drug), Y-27632–treated, and Blebbistatin-treated cells, stained with phalloidin (top) and Ser19-phospho-MLC (bottom). Scale bars are 10 µm.

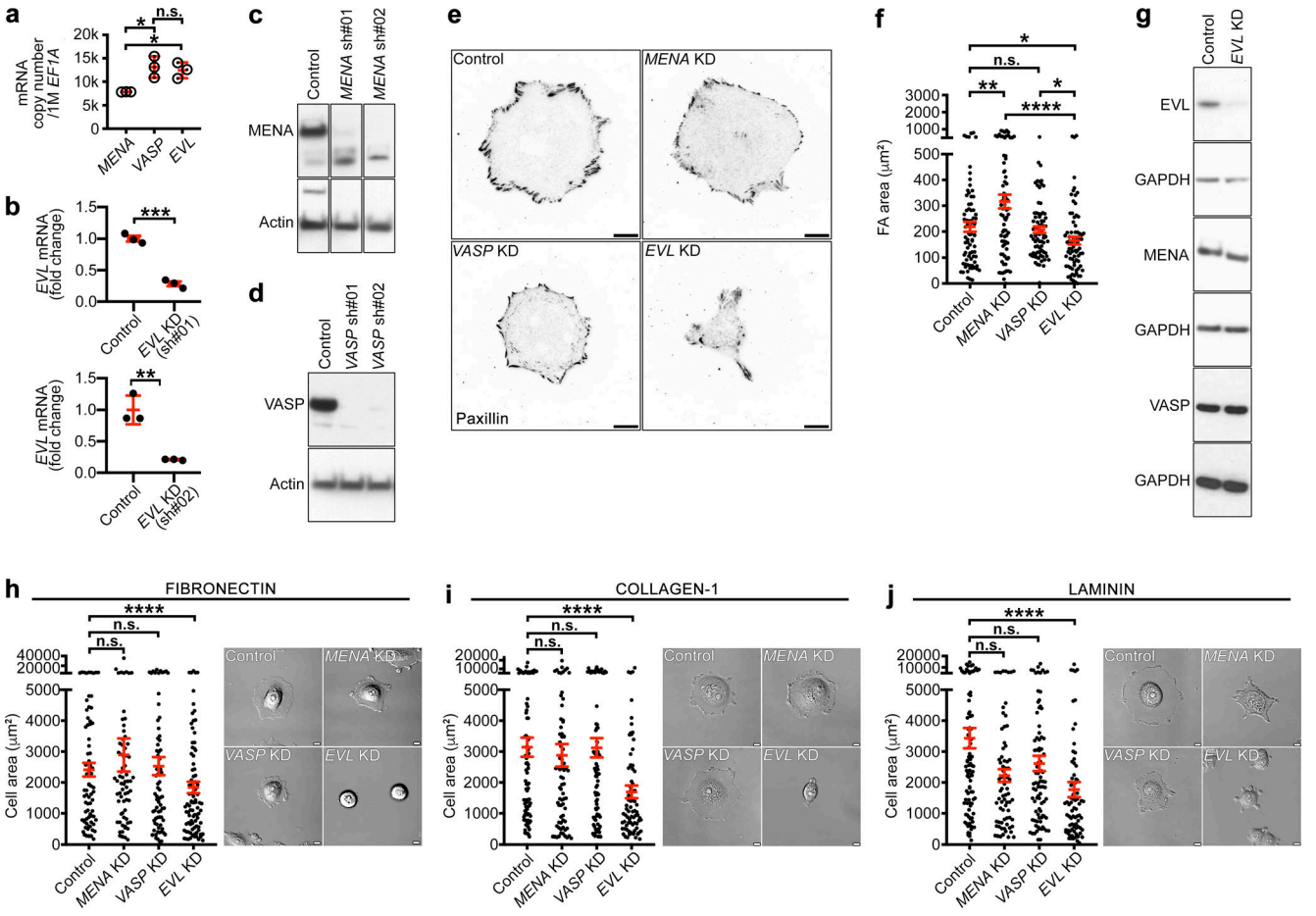

Figure S2. **EVL is required for cell-matrix adhesion. (a)** qPCR analysis of *MENA, VASP*, and *EVL* mRNA levels in control MCF7 cells relative to housekeeping gene *EEF1A1*. Data were collected from three independent experiments; all data points are shown (n = 3 per condition; P values were determined using two-tailed Student's t test; *, P ≤ 0.05; n.s., not significant; exact P values are found in Table S2; mean ± SD). **(b)** qPCR analysis of *EVL* mRNA levels in MCF7 cells infected with control (LKO) vector or *shEVL*. Data were collected from three independent experiments; all data points are shown (n = 3 per condition; P values were determined using two-tailed Student's t test; **, P ≤ 0.01; ***, P ≤ 0.001; n.s., not significant; exact P values are found in Table S2; mean ± SD). **(c)** Immunoblots of MCF7 cells infected with control (LKO) vector or *shMENA*. Top crop was probed with an antibody against MENA, and bottom crop was probed with an antibody against actin. **(d)** Immunoblots of MCF7 cells infected with control (LKO) vector or *shVASP*. Top crop was probed with an antibody against VASP, and bottom crop was probed with an antibody against actin. **(e)** Representative inverted TIRF images of paxillin staining in control (LKO vector), *MENA* KD, *VASP* KD, and *EVL* KD MCF7 cells. Scale bars are 10 µm. **(f)** Dot plot shows quantification of FA area. Data are collected from three independent experiments; all data points are shown (n ≥ 75 per condition; P values were determined using regression analysis; *, P ≤ 0.05; **, P ≤ 0.01; ****, P ≤ 0.0001; n.s., not significant; exact P values for all two-way comparisons are found in Table S3; mean ± SEM). **(g)** Immunoblots of control (LKO vector) and *EVL* KD MCF7 cells. Crops were probed with antibodies against EVL, MENA, or VASP and an antibody against GAPDH. **(h)** Representative images of control (LKO vector), *MENA* KD, *VASP* KD, and *EVL* KD MCF7 cells 24 h after plating on fibronectin. Scale bars are 10 µm. Dot plots show quantification of cell area. Data are collected from five independent experiments; all data points are shown (n ≥ 70 per condition; P values were determined using regression analysis; ****, P ≤ 0.0001; n.s., not significant; exact P values for all two-way comparisons are found in Table S3; mean ± SEM). **(i)** Representative images of control (LKO vector), *MENA* KD, *VASP* KD, and *EVL* KD MCF7 cells 24 h after plating on collagen. Scale bars are 10 µm. Dot plots show quantification of cell area. Data are collected from five independent experiments; all data points are shown (n ≥ 74 per condition; P values were determined using regression analysis; ****, P ≤ 0.0001; n.s., not significant; exact P values for all two-way comparisons are found in Table S3; mean ± SEM). **(j)** Representative images of control (LKO vector), *MENA* KD, *VASP* KD, and *EVL* KD MCF7 cells 24 h after plating on laminin. Scale bars are 10 µm. Dot plots show quantification of cell area. Data are collected from five independent experiments; all data points are shown (n ≥ 74 per condition; P values were determined using regression analysis; ****, P ≤ 0.0001; n.s., not significant; exact P values for all two-way comparisons are found in Table S3; mean ± SEM).

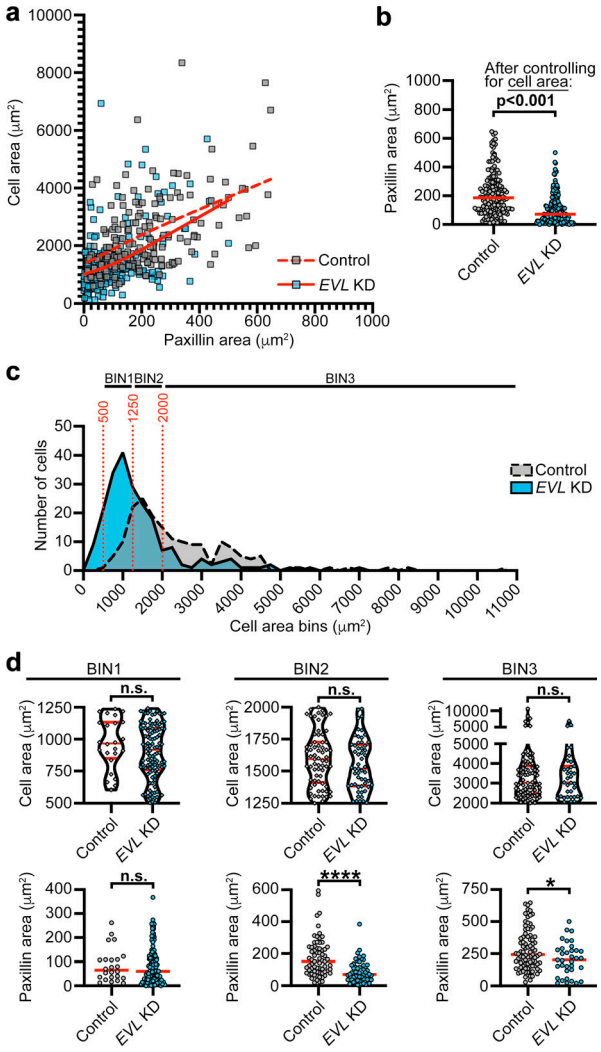

Figure S3. **FA area is reduced independently of cell spreading. (a)** Scatterplot showing paxillin area versus cell area. Spearman's rank correlation for LKO control r = 0.503, P < 0.0001; *EVL* KD r = 0.390, P < 0.0001. Dashed line and solid line are curve fits of all control (LKO vector) and *EVL* KD data points, respectively, using restricted cubic spline curve fitting. Data are collected from six independent experiments; all data points are shown (n = 177 LKO control, n = 214 *EVL* KD). **(b)** Paxillin area of control (LKO vector) and *EVL* KD cells. Red line denotes median. Statistical analysis performed by multiple regression analysis, controlling for experiment and cell area; exact P values are found in Table S2. Data are collected from six independent experiments; all data points are shown (n = 177 LKO control, n = 214 *EVL* KD). **(c)** Histogram of cell area bins showing number of cells per bin (BIN1, 500–1,250 μm²; BIN2, 1,250–2,000 μm²; BIN3, <2,000 μm²) and distribution of control (LKO vector) and *EVL* KD cells. Data are collected from six independent experiments; all data points are shown (n = 177 LKO control, n = 214 *EVL* KD). **(d)** Cell area (top row) and paxillin area (bottom row) of control (LKO vector) and *EVL* KD cells binned by cell area, red line denotes median, quartiles. P values were determined using Mann–Whitney *U* test; *, P ≤ 0.05; ****, P ≤ 0.0001; n.s., not significant; exact P values are found in Table S2.

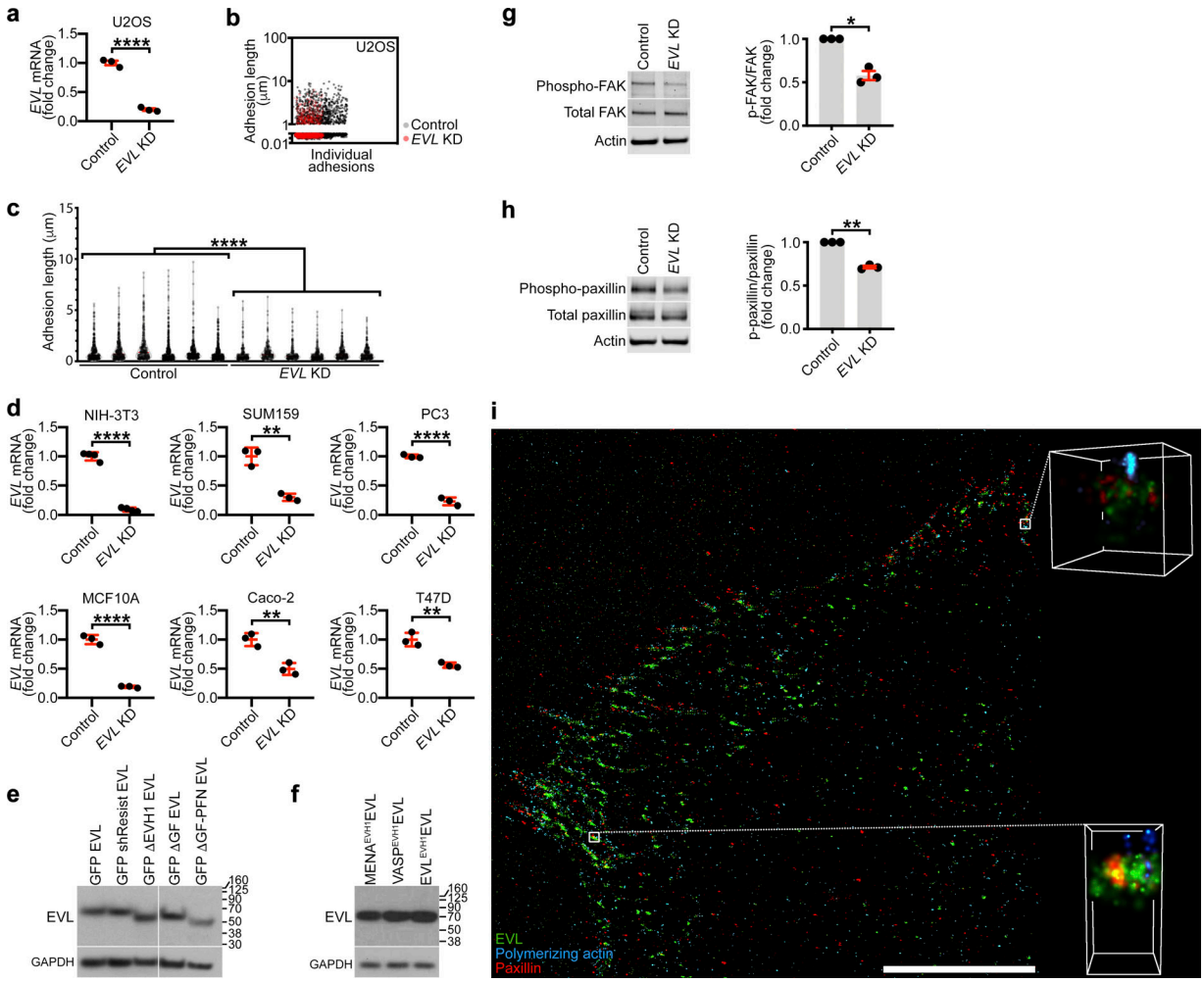

Figure S4. ***EVL* KD reduces FA maturation and mechanosensory signaling, and EVL localizes with sites of actin polymerization at FAs. (a)** qPCR analysis of *EVL* mRNA levels in U2OS cells infected with control (LKO) vector or *shEVL*. Data are collected from three independent experiments; all data points are shown (n = 3 per condition; P values were determined using two-tailed Student's t test; ****, P ≤ 0.0001; n.s., not significant; exact P values are found in Table S2; mean ± SD). **(b)** Scatter plot shows individual FA length measurements from control (LKO vector) and *EVL* KD cells. The lengths of >1,600 FAs from six cells per condition were measured; all data points are shown. **(c)** Volcano plot shows distribution of FA lengths in individual cells; all data points are shown (n ≥ 1,618 per condition; P values were determined using regression analysis; ****, P ≤ 0.0001; n.s., not significant, volcano plot shows median and quartiles of FA lengths; exact P values are found in Table S2). **(d)** qPCR analysis of *EVL* mRNA levels in cell line panel infected with control (LKO) vector or *shEVL*. Data are collected from three independent experiments per cell line, all data points are shown (n = 3 per condition; P values were determined using two-tailed Student's t test; **, P ≤ 0.01; ****, P ≤ 0.0001; n.s., not significant; exact P values are found in Table S2; mean ± SD). **(e)** Immunoblots of MCF7 cells infected with GFP-EVL, GFP-shResist EVL, GFP-ΔEVH1 EVL, GFP-ΔGF EVL, or GFP-ΔGF-PFN EVL. Top crop was probed with an antibody against EVL, and bottom crop was probed with an antibody against GAPDH. **(f)** Immunoblots of MCF7 cells infected with GFP-EVH1^{MENA}EVL, GFP-EVH1^{VASP}EVL, or GFP-EVH1^{EVL}EVL (same construct as GFP-shResist EVL). Top crop was probed with an antibody against EVL, and bottom crop was probed with an antibody against GAPDH. **(g)** Left: Immunoblots of control (LKO vector) and *EVL* KD MCF7 cells. Crops were probed with antibodies against Tyr397-phospho-FAK, total FAK, and actin. Right: Dot plot shows quantification of signal in control and *EVL* KD MCF7 cells. Data are collected from three independent experiments; all data points are shown (n = 3, P values were determined using two-tailed Student's t test; *, P ≤ 0.05; n.s., not significant; exact P values are found in Table S2; mean ± SEM). **(h)** Left: Immunoblots of control (LKO vector) and *EVL* KD MCF7 cells. Crops were probed with antibodies against Tyr118-phospho-paxillin, total paxillin, and actin. Right: Dot plot shows quantification of signal in control and *EVL* KD MCF7 cells. Data are collected from three independent experiments; all data points are shown (n = 3, P values were determined using two-tailed Student's t test; **, P ≤ 0.01; n.s., not significant; exact P values are found in Table S2; mean ± SEM). **(i)** Representative N-STORM image of GFP-EVL, labeled barbed ends, and paxillin staining from in situ actin polymerization assays in MCF7 cells. Scale bar is 10 μm. Top magnified cube is 3D view of N-STORM imaging of GFP-EVL, labeled barbed ends, and paxillin from top boxed inset. Cube is 1 μm^3. Bottom magnified cube is 3D view of N-STORM imaging of GFP-EVL, labeled barbed ends, and paxillin from bottom boxed inset. Cube is 500 nm in x and y and 1 μm in z.

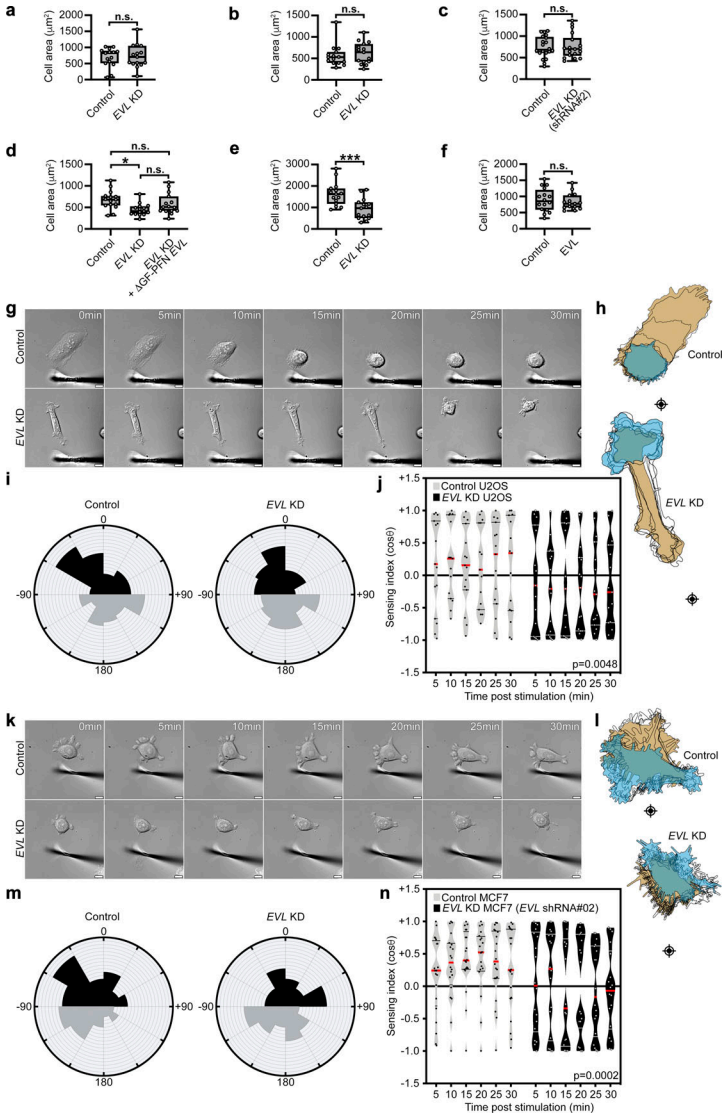

Figure S5. **Cell area measurements for all mechanically directed motility assays and analysis of mechanically directed motility in *EVL* KD cells. (a–f)** Box-and-whisker plots of cell areas at 0 min related to mechanically directed motility assays. All data points are shown; whiskers indicate minimum–maximum. **(a)** Cell areas from control or *EVL* KD MCF7 on 35-kPa gels, related to Fig. 5, a–d. Data are collected from six independent experiments (n = 15 per condition; P values were determined using two-tailed Student's t test). **(b)** Cell areas from control or *EVL* KD U2OS on 35-kPa gels, related to Fig. S5, g–j. Data are collected from four independent experiments (n = 15 per condition; P values were determined using two-tailed Student's t test). **(c)** Cell areas from control or *EVL* KD (shRNA#02) MCF7 on 35-kPa gels, related to Fig. S5, k–n. Data are collected from four independent experiments ($n \geq 18$ per condition; P values were determined using two-tailed Student's t test). **(d)** Cell areas from control + GFP, *EVL* KD + GFP, and *EVL* KD + GFP-ΔGF-PFN EVL MCF7, related to Fig. 5, h–k. Data are collected from three independent experiments (n = 15 per condition; P values were determined using one-way ANOVA). **(e)** Cell areas from control or *EVL* KD MCF7 on 8-kPa gels, related to Fig. 6, b–e. Data are collected from four independent experiments (n = 15 per condition; P values were determined using two-tailed Student's t test). **(f)** Cell areas from GFP or GFP-EVL in MV^{D7}, related to Fig. 7, a–d. Data are collected from five independent experiments ($n \geq 15$ per condition; P values were determined using two-tailed Student's t test). *, P ≤ 0.05; ***, P ≤ 0.001; n.s., not significant; exact P values are found in Tables S2 and S3. **(g–j)** Control (LKO vector) and *EVL* KD U2OS cells, plated on 35-kPa hydrogels, were mechanically stimulated. **(g)** Still images from representative time-lapse videos of control and *EVL* KD U2OS cells (Video 5). Scale bars are 10 µm. **(h)** Corresponding cell traces at 0, 5, 10, 15, 20, 25, and 30 min, with starting positions in tan and final positions in blue. Crosshairs denote micropipette positions. **(i)** Rose plots show cumulative turning angles for control and *EVL* KD U2OS cells. Black sectors denote turns in the direction of the force gradient, and gray sectors denote turns away from the force gradient. Data are collected from four independent experiments (n = 15 per condition). **(j)** Sensing indices of control and *EVL* KD U2OS cells over time. Two-way ANOVA shows a significant difference in sensing index between control and *EVL* KD U2OS cells (P = 0.0048). Data are collected from four independent experiments; all data points are shown (n = 15 per condition; violin plot shows median and quartiles of sensing indices). **(k–n)** Control (LKO vector) and *EVL* KD *(shRNA#02)* MCF7 cells, plated on 35-kPa hydrogels, were mechanically stimulated. **(k)** Still images from representative time-lapse videos of control and *EVL* KD *(shRNA#02)* cells (Video 6). Scale bars are 10 µm. **(l)** Corresponding cell traces at 0, 5, 10, 15, 20, 25, and 30 min, with starting positions in tan and final positions in blue. Crosshairs denote micropipette positions. **(m)** Rose plots show cumulative turning angles for control and *EVL* KD *(shRNA#02)* cells. Black sectors denote turns in the direction of the force gradient, and gray sectors denote turns away from the force gradient. Data are collected from four independent experiments ($n \geq 18$ per condition). **(n)** Sensing indices of control and *EVL* KD *(shRNA#02)* cells over time. Two-way ANOVA shows a significant difference in sensing index between control and *EVL* KD cells (P = 0.0002). Data are collected from four independent experiments; all data points are shown ($n \geq 18$ per condition; violin plot shows median and quartiles of sensing indices).

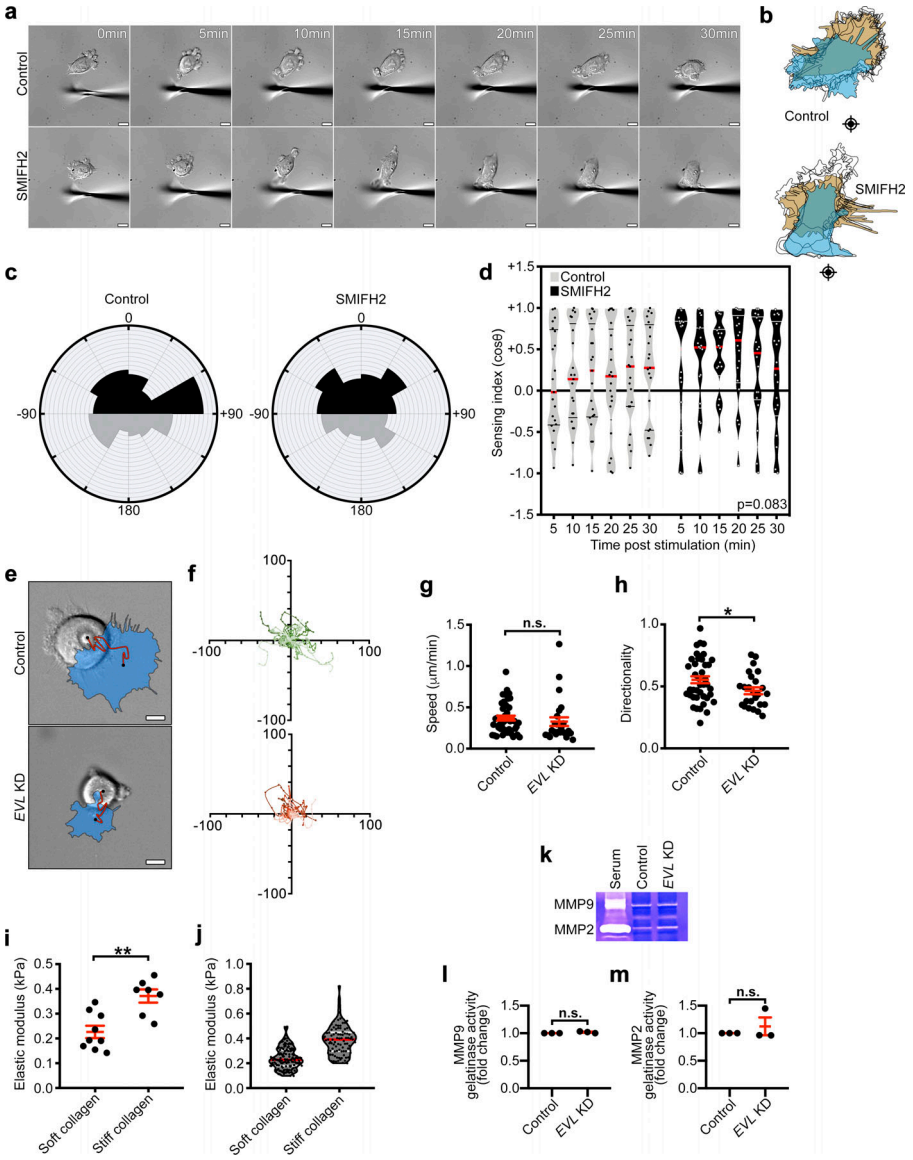

Figure S6. ***EVL* KD impairs directionality, but not random migration speed of cells or MMP activity. (a–d)** Control (no drug) and SMIFH2 (15 µM)-treated MCF7 cells, plated on 35-kPa hydrogels, were mechanically stimulated. **(a)** Still images from representative time-lapse videos of control and SMIFH2-treated cells (Video 8). Scale bars are 10 µm. **(b)** Corresponding cell traces at 0, 5, 10, 15, 20, 25, and 30 min, with starting positions in tan and final positions in blue. Crosshairs denote micropipette positions. **(c)** Rose plots show cumulative turning angles for control and SMIFH2 treated cells. Black sectors denote turns in the direction of the mechanical stimulus, and gray sectors denote turns away from the mechanical stimulus. Data are collected from six independent experiments ($n \geq 18$ per condition). **(d)** Sensing indices of control and SMIFH2-treated cells over time. Two-way ANOVA shows no significant difference in sensing index (P = 0.0827). Data are collected from six independent experiments; all data points are shown ($n \geq 18$ per condition; violin plot shows median and quartiles of sensing indices). **(e)** Representative DIC images of control (LKO vector) and *EVL* KD MCF7 cells on 35-kPa hydrogels. Red line denotes cell track, and blue binary denotes the final position of the cell. Scale bars are 10 µm. **(f)** Cell tracks of all analyzed cells; top tracks are control, and bottom tracks are *EVL* KD (axes are in µm). **(g)** Dot plot shows quantification of random migration speed. Data are collected from three independent experiments; all data points are shown ($n \geq 25$ per condition; P values were determined using regression analysis; n.s., not significant; exact P values are found in Table S2; mean ± SEM). **(h)** Dot plot shows quantification of cell directionality averaged from time intervals ≤2 h. Data are collected from three independent experiments; all data points are shown ($n \geq 25$ per condition; P values were determined using regression analysis; *, $P \leq 0.05$; n.s., not significant; exact P values are found in Table S2; mean ± SEM). **(i and j)** Atomic force microscope–based nano-indentation of collagen matrices. **(i)** Dot plot shows quantification of elastic moduli of soft and stiff collagen gels. Each dot represents the average measurements taken in a separate area of the gel. Data are collected from three independent experiments; all data points are shown ($n \geq 7$ per condition; P values were determined using two-tailed Student's *t* test; **, $P \leq 0.01$; n.s., not significant; exact P values are found in Table S2; mean ± SEM). **(j)** Violin plot shows distribution of individual indentation measurements taken from all areas of each collagen gel. Data are collected from three independent experiments; all data points are shown ($n \geq 89$ per condition; violin plot shows median and quartiles of elastic moduli). **(k–m)** Gelatin zymography of control (LKO vector) and *EVL* KD MCF7 cells. **(k)** Representative gelatin zymogram (enhanced image) showing gelatinase activity of 5% FBS with lysates from control and *EVL* KD cells. **(l and m)** Dot plots show fold change in gelatinase activity between control and *EVL* KD cells for band corresponding to MMP9 (l), and band corresponding to MMP2 (m). Data are collected from three independent experiments; all data points are shown ($n = 3$ per condition; P values were determined using two-tailed Student's *t* test; *, $P \leq 0.05$; **, $P \leq 0.01$; ***, $P \leq 0.001$; ****, $P \leq 0.0001$; n.s., not significant; exact P values are found in Table S2; mean ± SEM).

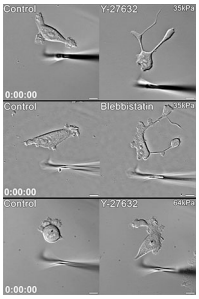

Video 1. **Mechano-stimulated control and Y-27632– or Blebbistatin-treated MCF7 cells on 35-kPa hydrogel.** Top: Time-lapse video of mechano-stimulated control and Y-27632–treated MCF7 cells on 35-kPa hydrogel. DIC images were acquired at 1 frame/s. Scale bar is 10 µm. Middle: Time-lapse video of mechano-stimulated control and Blebbistatin-treated MCF7 cells on 35-kPa hydrogel. DIC images were acquired at 1 frame/s. Scale bar is 10 µm. Bottom: Time-lapse video of mechano-stimulated control and Y-27632–treated MCF7 cells on 64-kPa hydrogel. DIC images were acquired at 1 frame/s. Scale bar is 10 µm.

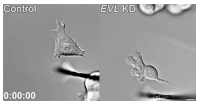

Video 2. **Time-lapse video of mechano-stimulated control and *EVL* KD MCF7 cells on 35-kPa hydrogel.** DIC images were acquired at 1 frame/s. Scale bar is 10 µm.

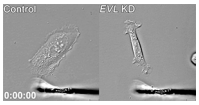

Video 3. **Time-lapse video of mechano-stimulated control and *EVL* KD U2OS cells on 35-kPa hydrogel.** DIC images were acquired at 1 frame/s. Scale bar is 10 µm.

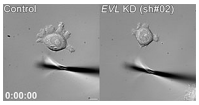

Video 4. **Time-lapse video of mechano-stimulated control and *EVL* KD (shRNA #02) MCF7 cells on 35-kPa hydrogel.** DIC images were acquired at 1 frame/s. Scale bar is 10 µm.

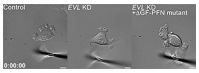

Video 5. **Time-lapse video of mechano-stimulated control + GFP, *EVL* KD + GFP, and *EVL* KD + GFP-ΔGF-PFN EVL MCF7 cells on 35-kPa hydrogel.** DIC images were acquired at 1 frame/s. Scale bar is 10 µm.

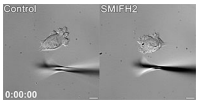

Video 6. **Time-lapse video of mechano-stimulated control and SMIFH2-treated MCF7 cells on 35-kPa hydrogel.** DIC images were acquired at 1 frame/s. Scale bar is 10 µm.

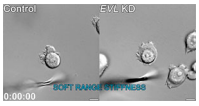

Video 7. **Time-lapse video of mechano-stimulated control and *EVL* KD MCF7 cells on 8-kPa hydrogel.** DIC images were acquired at 1 frame/s. Scale bar is 10 µm.

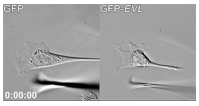

Video 8. **Time-lapse video of mechano-stimulated GFP and GFP-EVL expressing MV^{D7}cells on 35-kPa hydrogel.** DIC images were acquired at 1 frame/s. Scale bar is 10 µm.

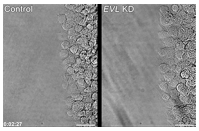

Video 9. **Time-lapse video of control and *EVL* KD U2OS cells during durotactic invasion.** DIC images were acquired at 1 frame/10 min. Scale bar is 50 µm.

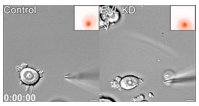

Video 10. **Time-lapse video of chemo-stimulated control and *EVL* KD MCF7 cells.** DIC images were acquired at 1 frame/s. Scale bar is 10 µm.